



## A Characteristic-based Numerical Simulation of Water-titanium Dioxide Nano-fluid in Closed Domains

T. Adibi<sup>a</sup>, S. E. Razavi<sup>b</sup>, O. Adibi<sup>c</sup>

<sup>a</sup> Department of Mechanical Engineering, University of Bonab, Bonab, Iran

<sup>b</sup> School of Mechanical Engineering, University of Tabriz, Tabriz, Iran

<sup>c</sup> School of Mechanical Engineering, Sharif University of Technology, Tehran, Iran

### PAPER INFO

#### Paper history:

Received 19 September 2019

Received in revised form 04 November 2019

Accepted 08 November 2019

#### Keywords:

Titanium Dioxide

Nano-fluid

Nusselt Number

Friction Factor

Numerical Method

### ABSTRACT

A new characteristic-based method is developed and used for solving the mixed and forced convection problems. The nano-fluid flow with heat transfer is simulated with a novel characteristic-based scheme in closed domains with different aspect ratios. For this purpose, a FORTRAN code has been written and developed. Water as a pure fluid and water-titanium dioxide as a nano-fluid were considered. The governing equations are solved by the finite volume utilizing a characteristic-based scheme for the convective fluxes. The simulation is done at Grashof numbers from 100 to  $10^4$ , Reynolds numbers from 100 to 1000, and volume fractions of nano-particles from 0% to 10%. Streamlines, isotherms, friction factor, and mean Nusselt number are obtained in various conditions. The convective behavior of nano-fluid is explored as a function of several parameters, such as Grashof number and geometrical parameters. Results indicate that the mean Nusselt number for the nanofluid is up to 23% more than that of pure water.

doi: 10.5829/ije.2020.33.01a.18

### NOMENCLATURE

C	The volume fraction of nanoparticle	u, v	X, y velocity components
$C_p$	Specific heat in constant pressure(J/kg/K)	Re	Reynolds number
D	Diameter (m)	T	Temperature
f	Friction factor	x, y	Coordinates
$\bar{f}$	Mean friction factor	<b>Greek Symbols</b>	
g	Gravitational acceleration ( $m/s^2$ )	$\beta$	Artificial compressibility coefficient
Gr	Grashof number	$\beta_{ex}$	Thermal expansion coefficient ( $K^{-1}$ )
k	Thermal conductivity (W/m/K)	$\mu$	Coefficient of viscosity (kg/m/s)
M	Number of cells in x-direction	$\nu$	Kinematic viscosity ( $m^2/s$ )
N	Number of cells in the y-direction	$\rho$	Density ( $kg/m^3$ )
$N_c$	Thermal conductivity parameter	Subscripts	
Nu	Local Nusselt number	ref	Reference
$\bar{Nu}$	Mean Nusselt number	bf	Body fluid
$N_v$	Dynamic viscous parameter	nf	Nano-fluid
p	Pressure	p	Particle
Pr	Prandtl number		

## 1. INTRODUCTION

Increasing the heat transfer rate has been a significant issue for investigators. The main goal is to improve the thermophysical properties of convective heat transfer.

Nano-fluids have features that make them beneficial for various applications of heat transfer, including microelectronics, fuel cells, pharmaceutical processes, and so forth. They showed an enhanced heat transfer rate compared to base fluid [1]. Knowledge of the rheological

\*Corresponding Author Email: Tohidadibi@bonabu.ac.ir (T. Adibi)

behavior of nano-fluids is critical in determining their appropriateness for convective heat transfer applications. Mohebbi et al. [2] performed a numerical study on laminar forced convection with nano-fluid. They used CuO, Al<sub>2</sub>O<sub>3</sub>, and TiO<sub>2</sub> nano-particles with water along with the Lattice-Boltzmann method. Reynolds number is considered from 10 to 70, and nanofluid concentration is considered up to 0.05. Yigit et al. [3] simulated mixed convection with nanofluid numerically. Water- alumina was considered, and simulations were done for Reynolds numbers from 500 to 3000, Richardson numbers from 0 to 1, and nanoparticle volume fractions up to 5%. Astanina et al. [4] performed a numerical study on Al<sub>2</sub>O<sub>3</sub>-water nano-fluid. Mixed convection was simulated at Richardson numbers from 0.01 to 10 nanoparticle volume fractions up to 4%. Alsabery et al. [5] studied mixed convection with nano-fluid numerically. A finite volume method was used, and simulations were done for nanoparticles volume fraction up to 4%, Reynolds numbers from 1 to 500, and Richardson number from 0.01 to 100. Abolbashari et al. [6] investigated the influence of different nano-fluids on the heat transfer rate numerically. Copper, copper oxide, aluminum oxide, and titanium dioxide were used as nano-particles with water.

The natural convection in the cavity was simulated. Mahmoodi [7] studied the natural convection with the nano-fluids in the cavity flow numerically. He used the SIMPLER algorithm. Different nano-particle with water was considered. Rahmati and Tahery [8] simulated the laminar natural convection in the cavity flow numerically. They studied water-TiO<sub>2</sub> nano-fluid with Lattice- Boltzmann method. An obstacle was considered in different parts of the cavity. Heydari et al. [9] solved three-dimensional nano-fluid flow in heat exchanger numerically. They used Al<sub>2</sub>O<sub>3</sub>, CuO, Fe<sub>2</sub>O<sub>3</sub>, Cu, Fe, SiO<sub>2</sub>, and Au with water and ethylene glycol. Razeghi et al. [10] simulated incompressible nano-fluid flow with Al<sub>2</sub>O<sub>3</sub>-water numerically. Single-phase and multi-phase approach are compared. Results showed, nano-particles concentration decreases entropy generation due to heat transfer and enhances entropy generation due to fluid friction. Mahdy [11] simulated incompressible nano-fluid flow with non-Newtonian nano-fluid. The effects of the power-law viscosity index and the similarity exponent on the heat transfer characteristics had been studied. Bakhshi et al. [12] Studied a heat exchanger experimentally. Al<sub>2</sub>O<sub>3</sub>-water used as a nano-fluid. Akbarzadeh et al. [13] did an experimental study on forced convection in a radiator of a car. SiO<sub>2</sub> nano-particle used to improve the heat transfer rate. Results showed that Nusselt number increases with an increase of liquid inlet temperature, nanoparticle volume fraction and Reynolds number. Kumar et al. [14] studied the effect of nano-fluid on Nusselt number and heat transfer rate. TiO<sub>2</sub> with water and glycol is used, and simulations are done for incompressible turbulent flow. Gnanavel et

al. [15] simulated laminar and turbulent nanoflow with different nanofluids numerically. Nanofluid heat transfer characteristics were obtained and compared with each other and the best one was determined. Sarkar et al.[16] used water-TiO<sub>2</sub> nano-fluid for coolant purposes. Results showed that the heat transfer rate increases 19% for the nanofluid with 40ppm of TiO<sub>2</sub> nanoparticle.

In present work, water and water-TiO<sub>2</sub> nano-fluid with different volume fractions were considered. The simulations are done for a wide range of the Grashof numbers, the Reynolds numbers, and the aspect ratios of the cavity. The cavity flow is a benchmark for numerical simulations [17], and actually, the smooth surfaces can be substituted by surfaces embedding cavities, which drastically could enhance the convective heat transfer coefficient. The convective terms in the governing equation are discretized by a characteristic-based scheme that was introduced by the authors [18-20].

## 2. THE GOVERNING EQUATIONS AND NUMERICAL PROCEDURE

Nano-fluids can be assumed to be single-phase fluids in a numerical study where the physical properties of nano-fluids are taken as a function of properties of both based-fluid and nano-particle. The governing equations for two-dimensional nano-fluid with heat transfer in the dimensionless[19] form are

$$\begin{aligned} \frac{1}{\beta} \frac{\partial p}{\partial t} + \frac{\partial u}{\partial x} + \frac{\partial v}{\partial y} &= 0; \\ \frac{\partial u}{\partial t} + u \frac{\partial u}{\partial x} + v \frac{\partial u}{\partial y} &= -\frac{\rho_{bf}}{\rho_{nf}} \frac{\partial p}{\partial x} + \frac{\rho_{bf} \mu_{nf}}{\rho_{nf} \mu_{bf}} \frac{1}{Re} \left( \frac{\partial^2 u}{\partial x^2} + \frac{\partial^2 u}{\partial y^2} \right); \\ \frac{\partial v}{\partial t} + u \frac{\partial v}{\partial x} + v \frac{\partial v}{\partial y} &= -\frac{\rho_{bf}}{\rho_{nf}} \frac{\partial p}{\partial y} + \frac{\rho_{bf} \mu_{nf}}{\rho_{nf} \mu_{bf}} \frac{1}{Re} \left( \frac{\partial^2 v}{\partial x^2} + \frac{\partial^2 v}{\partial y^2} \right) - \frac{Gr}{Re^2} \beta_{nf} T; \\ \frac{\partial T}{\partial t} + u \frac{\partial T}{\partial x} + v \frac{\partial T}{\partial y} &= \frac{(\rho C_p)_{bf} k_{nf}}{(\rho C_p)_{nf} k_{bf}} \frac{1}{Pr} \left( \frac{\partial^2 T}{\partial x^2} + \frac{\partial^2 T}{\partial y^2} \right). \end{aligned} \quad (1)$$

where,  $\beta$  is the artificial compressibility, and one has the following

$$\begin{aligned} Re &= \frac{V_{ref} L_{ref}}{\vartheta_{bf}}; \quad Pr = \frac{(C_p)_{bf} \mu_{bf}}{k_{bf}}; \\ Gr &= \frac{(\beta_{ex})_{bf} g (T_{ref1} - T_{ref2}) L_{ref}^2}{\vartheta_{bf}^2} \end{aligned} \quad (2)$$

Hence,  $L_{ref}$  is the cavity length and  $V_{ref}$  is the velocity of the upper wall. Also,  $T_{ref1}$  and  $T_{ref2}$  show the temperatures of the upper and the lower walls. The properties of water, TiO<sub>2</sub>, and nano-fluid were obtained from literature [21]. The following relations are used as nano-fluid relations [21]:

$$\frac{\rho_{nf}}{\rho_{bf}} = 1 - C + C \frac{\rho_p}{\rho_{bf}}; \frac{\mu_{nf}}{\mu_{bf}} = 1 + Nv \times C;$$

$$\frac{(\rho C_{cp})_{bf}}{(\rho C_{cp})_{nf}} = (1 - C) + C \frac{(\rho C_{cp})_p}{(\rho C_{cp})_{bf}};$$

$$\frac{k_{nf}}{k_{bf}} = 1 + Nc \times C; \frac{\beta_{nf}}{\beta_{bf}} = \frac{\rho_{bf}}{\rho_{nf}} \left[ (1 - C) + C \frac{(\rho\beta)_p}{(\rho\beta)_{bf}} \right]$$

(3)

The governing equations are discretized by the finite volume method, where fifth-order Rung-Kutta was used for time discretization. The convective fluxes were calculated by the characteristic-based method introduced by the authors' previous works [19, 20]. The boundary conditions are applied as in Figure 1.

### 3. RESULTS AND DISCUSSION

A FORTRAN-95 code has been written to simulate the nanofluid flow. Grid independence is displayed in Figure 2. A grid with 80×80 cells is chosen. The present code was run with various grid sizes at this range. No special deviation in results was observed. It would be possible, also, to work with 60×60 grid cells, however for more safety purpose, the higher was taken. The code was capable of capturing the flow details property and predicting the heat transfer characteristics.

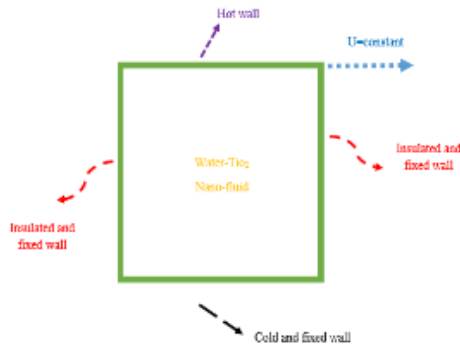


Figure 1. Cavity with water\_TiO<sub>2</sub> nano-fluid and corresponding boundary conditions

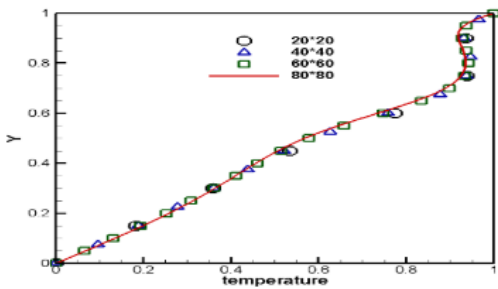


Figure 2. Grid independence at Re=100, Gr=10000, and C=10% (Temperature variation on the vertical centreline of cavity)

The results of the written code are validated with that of Iwatsu et al. [22] and are shown in Figure 3. As it is observed, good agreement is between the present results and that of Iwatsu et al. The friction factor is calculated as follows [21] :

$$f = \frac{2}{Re} \frac{\mu_{nf}}{\mu_{bf}} \frac{\partial u}{\partial y} = \frac{2}{Re} \frac{\mu_{nf}}{\mu_{bf}} \frac{u_2 - u_1}{y_2 - y_1}$$

(4)

The friction factor is shown in Figure 4 at the lower wall and in Figure 5 at the upper wall for Gr=1000 and Re=300. The shear stress near the walls raises, adding nano-particle to the fluid. As a result, the friction factor increases. The friction factor at the upper wall is more than the lower wall. The upper wall moves at a constant velocity, so the velocity gradient is high near the upper wall. The velocity of nano-fluid is high of the lower part is negative because of a formed vortex in the cavity. As

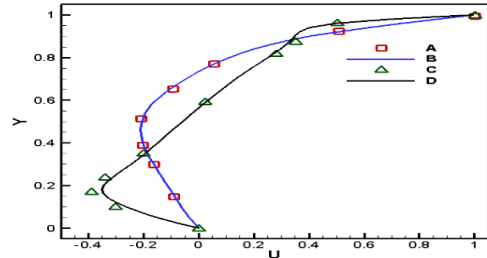


Figure 3. Comparison of results with that of Iwatsu et al. results at Pr=0.71, Gr=100 [22]. A) Iwatsu et al. results for Re=100, B) Present results for Re=100, C) Iwatsu results for Re=1000, D) Present results for Re=1000(velocity variation on the vertical centreline of the cavity)

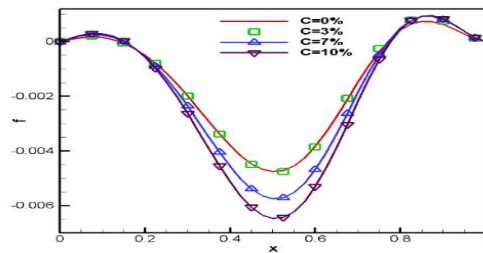


Figure 4. The behavior of friction factors for the lower wall for various concentrations at Gr=1000, Re=300

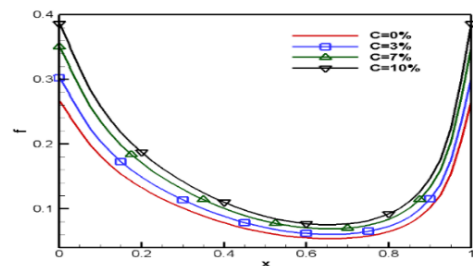


Figure 5. Comparison of friction factors for the upper wall for different concentrations at Gr=1000 and Re=300

a result, the friction factor for main part of the lower wall is negative. It is positive in small part because of small vortices. The lower wall experiences two maximums and one minimum due to the explained fact. The upper wall experience one minimum due to the fact that the velocity gradient is low in the middle part because this part is far from the left and right walls.

The Nusselt number is obtained by the following expression [21]

$$Nu = \frac{k_{nf} \partial T}{k_{bf} \partial y} = \frac{k_{nf} T_2 - T_1}{k_{bf} y_2 - y_1} \tag{5}$$

The obtained Nusselt numbers are shown in Figures 6 and 7 for Gr=1000 and Re=300. The Nusselt number for the nano-fluid is more than that of pure fluid, and it increases by the volume fraction. The upper wall moves right at the constant velocity. As a result, it helps to increase the heat transfer rate at the upper wall. Hence, the Nusselt number at the upper wall is more than the Nusselt number at the lower wall. Nusselt number variation is complicated at the lower wall. It is affected by different parameters such as vortex direction, left, and right thermal boundary conditions. As a result, the Nusselt number variation diagram has a maximum and a minimum in the middle part of the lower wall. In the upper part, the vortex direction forced cold nano-fluid to the left section. Consequently, the gradient of temperature variation and Nusselt number are high in this part. They decrease from left to right. The velocity of nano-fluid is positive in the upper parts and is negative in

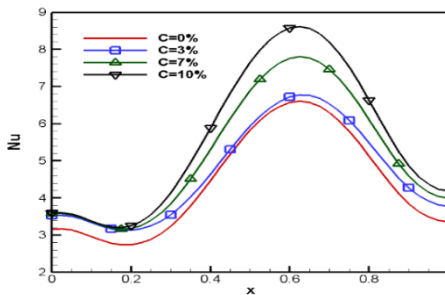


Figure 6. Nusselt number distribution at the lower wall for various concentrations and Gr=1000 and Re=300

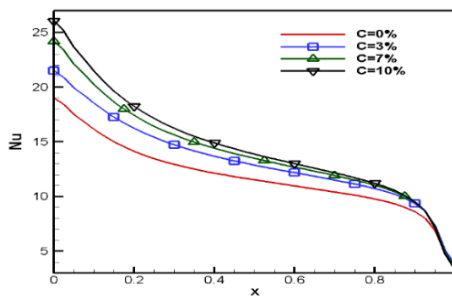


Figure 7. Nusselt number distribution at the upper wall for multiple concentrations and Gr=1000 and Re=300

the lower portion according to the vortex direction, but the temperature of nano-fluid is between upper and lower walls temperature and is not negative in any parts. As a result, the Nusselt number is positive in the upper and lower walls.

The mean friction factor and mean Nusselt number are obtained from following expression:

$$\begin{aligned} \bar{f} &= \int_0^1 f \, dx = \frac{1}{M} \sum_{i=1}^M f_i; \\ \overline{Nu} &= \int_0^1 Nu \, dx = \frac{1}{M} \sum_{i=1}^M Nu_i \end{aligned} \tag{6}$$

The mean friction factor and the mean Nusselt number at Gr=1000 and Re=300 are calculated by Equations (6) and shown in Table 1. The  $\overline{Nu}$  for the nano-fluid with a 10% volume fraction is 23% more than that of pure fluid at the upper wall. This is 19% at the lower wall. The  $\bar{f}$  for the nano-fluid with a 10% volume fraction is 42% more than that of pure fluid at the upper wall. It is 36% at the lower wall. Because of nano-particle effects, the effective viscosity and conductivity for nano-fluid are more than those of pure fluid. Consequently,  $\bar{f}$  and  $\overline{Nu}$  is more in nano-fluids. The friction factor and Nusselt number of the upper wall are effected higher than the down wall by nano-particle.

In this part, the influence of the Grashof number on the nano-fluid flow properties is surveyed. The streamlines are shown in Figure 8 for different Grashof numbers at C=10% and Re=200. There is one primary vortex at the low Grashof number, but there are two primary vortices at the high Grashof numbers. The second vortex is formed and becomes more significant at high Grashof numbers. In other words, the density of the nano-fluid changes more at high Grashof numbers. The low-density parts of nano-fluid moves upward and vice versa. Hence, the second vortex is formed.

TABLE 1. The mean friction factor and the mean Nusselt number at Gr=1000 and Re=300

-	$\overline{Nu}$		$\bar{f}$	
	Upper wall	Lower wall	Upper wall	Lower wall
C=0%	11.83	4.71	0.111	-1.48E-3
C=3%	13.27	4.70	0.125	-1.45E-3
C=7%	14.04	5.20	0.144	-1.77E-3
C=10%	14.56	5.61	0.158	-2.02E-3

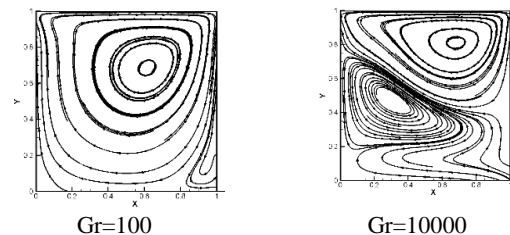


Figure 8. The streamlines for low and high Grashof numbers at C=10% and Re=200

The  $\bar{f}$  at upper and lower walls are obtained and displayed in Table 2. The influence of Grashof number on the  $\bar{f}$  at upper wall is negligible. The  $\bar{f}$  at lower wall decreases as the Grashof number increases due to shear stress reduction. The  $\overline{Nu}$  at the upper and the lower walls is calculated and shown in Table 2. The  $\overline{Nu}$  is high in low Grashof numbers at the upper and the lower walls.

In this section, the cavity flow with nano-fluid is simulated for different aspect ratios. The isotherms and streamlines are displayed at  $\frac{W}{L} = 2$ . Two vortices have been formed in this case. In this situation, the upper and lower walls are far from each other. The isotherms in the lower parts are parallel to each other. The influence of forced convection is negligible, and natural convection prevails.

The  $\bar{f}$  at upper and lower walls are obtained and displayed in Table 3 for  $C=10\%$ ,  $Re=100$ , and  $Gr=1000$ . The  $\bar{f}$  is high for low aspect ratios at the upper and the lower walls. Also the  $\overline{Nu}$  is high at low aspect ratios at the upper and the lower walls. As it is observed in Table 3,  $f$  and  $Nu$  for lower wall increase faster than them for the upper wall by aspect ratio reduction. At low aspect ratios, the distance between the upper and lower wall is less, and upper wall force nano-fluid to lower part easily; therefore, nano-fluid with high temperature and velocity move downward. As a result, the heat transfer rate and shear stress increase in the lower wall. Consequently,  $f$  and  $Nu$  rise in the lower wall too.

TABLE 2. The mean friction factor and the mean Nusselt number at  $C=10\%$  and  $Re=200$

-	$\overline{Nu}$		$\bar{f}$	
	Upper wall	Lower wall	Upper wall	Lower wall
$Gr=10^2$	13.17	5.05	0.222	-3.65E-3
$Gr=10^3$	12.79	4.56	0.222	-1.66E-3
$Gr=10^4$	6.49	3.13	0.233	-1.58E-3

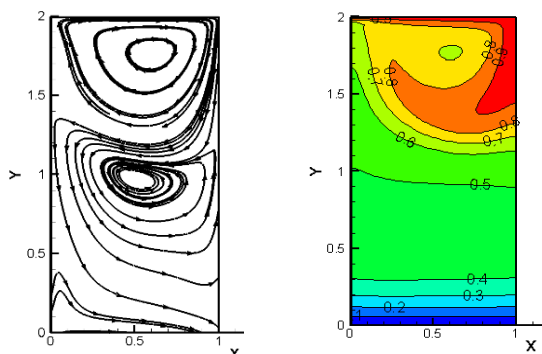


Figure 9. Streamlines(left) and Isotherms(right) at  $Gr=1000$ ,  $Re=100$ , and  $C=10\%$

TABLE 3. The mean friction factor and the mean Nusselt number at  $C=10\%$ ,  $Re=100$ , and  $Gr=1000$

-	$\overline{Nu}$		$\bar{f}$	
	Upper wall	Lower wall	Upper wall	Lower wall
$W/L=0.5$	13.10	9.04	0.532	-5.49E-02
$W/L=0.75$	11.44	5.35	0.500	-1.26E-02
$W/L=1.0$	8.67	3.22	0.416	-1.33E-04
$W/L=2.0$	7.17	2.51	0.413	1.19E-03
$W/L=4.0$	3.47	1.81	0.317	-4.42E-04

4. CONCLUSION

A novel characteristic-based method was developed and used for solving the mixed and forced convection problems. Incompressible two-dimensional flow with heat transfer in squared and non-squared cavities are simulated numerically. The water as a pure fluid, and the water -titanium dioxide nano-fluid were compared. The mean Nusselt is high for nano-fluids up to 23%, but at the same time, adding nano-particle to the base fluid raises the friction factor up to 42%. The mean Nusselt number increases when the Grashof number is lowered at nano-fluid flow. The mean Nusselt number becomes half when the Grashof number grows one hundred times. The mean Nusselt number rises when the aspect ratio is lowered at nano-fluid flow. The mean Nusselt number becomes half when the aspect ratio of the cavity increaseb by 2 folds.

5. REFERENCES

1. Kakaç, S. and Pramuanjaroenkij, A., "Review of convective heat transfer enhancement with nanofluids", *International Journal of Heat and Mass Transfer*, Vol. 52, No. 13, (2009), 3187-3196.
2. Mohebbi, R., Rashidi, M.M., Izadi, M., Sidik, N.A.C. and Xian, H.W., "Forced convection of nanofluids in an extended surfaces channel using lattice Boltzmann method", *International Journal of Heat and Mass Transfer*, Vol. 117, (2018), 1291-1303.
3. Yigit, S., Baruah, P. and Chakraborty, N., "Laminar mixed convection of water-based alumina nanofluid in a cylindrical enclosure with a rotating end wall: A numerical investigation", *Heat Transfer Engineering*, (2019), 1-14. <https://doi.org/10.1080/01457632.2018.1557939>
4. Astanina, M.S., Sheremet, M.A., Oztop, H.F. and Abu-Hamdeh, N., "Mixed convection of  $al_2o_3$ -water nanofluid in a lid-driven cavity having two porous layers", *International Journal of Heat and Mass Transfer*, Vol. 118, (2018), 527-537.
5. Alsabery, A.I., Ismael, M.A., Chamkha, A.J. and Hashim, I., "Mixed convection of  $al_2o_3$ -water nanofluid in a double lid-driven square cavity with a solid inner insert using buongiorno's two-phase model", *International Journal of Heat and Mass Transfer*, Vol. 119, (2018), 939-961.
6. Abolbashari, M.H., Freidoonimehr, N., Nazari, F. and Rashidi, M.M., "Entropy analysis for an unsteady mhd flow past a

- stretching permeable surface in nano-fluid", *Powder Technology*, Vol. 267, (2014), 256-267.
7. Mahmoodi, M., "Numerical simulation of free convection of nanofluid in a square cavity with an inside heater", *International Journal of Thermal Sciences*, Vol. 50, No. 11, (2011), 2161-2175.
  8. Rahmati, A.R. and Tahery, A.A., "Numerical study of nanofluid natural convection in a square cavity with a hot obstacle using lattice boltzmann method", *Alexandria Engineering Journal*, Vol. 57, No. 3, (2018), 1271-1286.
  9. Heydari, A., Shateri, M. and Sanjari, S., "Numerical analysis of a small size baffled shell-and-tube heat exchanger using different nano-fluids", *Heat Transfer Engineering*, Vol. 39, No. 2, (2018), 141-153.
  10. Razeghi, A., Mirzaee, I., Abbasalizadeh, M. and Soltanipour, H., "Al<sub>2</sub>O<sub>3</sub>/water nano-fluid forced convective flow in a rectangular curved micro-channel: First and second law analysis, single-phase and multi-phase approach", *Journal of the Brazilian Society of Mechanical Sciences and Engineering*, Vol. 39, No. 6, (2017), 2307-2318.
  11. Mahdy, A., "Non-newtonian nanofluid free convection flow subject to mixed thermal boundary conditions about a vertical cone", *Journal of the Brazilian Society of Mechanical Sciences and Engineering*, Vol. 36, No. 4, (2014), 951-960.
  12. Bakhshi, s.r., Borhani, G.h., Mehdikhani, B. and Baharvandi, H.r., "Synthesis of tantalum carbide/boride nano composite powders by mechanochemical method", *International Journal of Engineering, Tansaction B: Applications*, Vol. 27, No. 5, (2014), 769-774.
  13. Akbarzade, S., Sedighi, K., Farhadi, M. and ebrahimi, m., "Experimental investigation of force convection heat transfer in a car radiator filled with SiO<sub>2</sub>-water nanofluid", *International Journal of Engineering, Transactions B: Applications*, Vol. 27, No. 2, (2014), 333-340.
  14. Kumar, s., Hassan, S.B., Sharma, K. and Baheta, A., "Heat transfer coefficients investigation for TiO<sub>2</sub> based nanofluids", *International Journal of Engineering, Tansaction A: Basics*, Vol.32, No. 10, (2019): 1491-1496.
  15. Gnanavel, C., Saravanan, R. and Chandrasekaran, M., "Heat transfer enhancement through nano-fluids and twisted tape insert with rectangular cut on its rib in a double pipe heat exchanger", *Materials Today: Proceedings*, (2019). <https://doi.org/10.1016/j.matpr.2019.07.606>
  16. Sarkar, I., Chakraborty, S., Roshan, A., Behera, D.K., Pal, S.K. and Chakraborty, S., "Application of tio<sub>2</sub> nanofluid-based coolant for jet impingement quenching of a hot steel plate", *Experimental Heat Transfer*, Vol. 32, No. 4, (2019), 322-336.
  17. Adibi, T., Adibi, O. and Razavi, S.E., "A characteristic-based solution of forced and free convection in closed domains with emphasis on various fluids ", *International Journal of Engineering, Tansaction A: Basics*, Vol. 32, No. 10, (2019), 1679-1685.
  18. Adibi, T., "Three-dimensional characteristic approach for incompressible thermo-flows and influence of artificial compressibility parameter", *Journal of Computational & Applied Research in Mechanical Engineering*, Vol. 8, No. 2, (2019), 223-234.
  19. Adibi, T. and Razavi, S.E., "A new characteristic approach for incompressible thermo-flow in cartesian and non-cartesian grids", *International Journal for Numerical Methods in Fluids*, Vol. 79, No. 8, (2015), 371-393.
  20. Razavi, S.E. and Adibi, T., "A novel multidimensional characteristic modeling of incompressible convective heat transfer", *Journal of Applied Fluid Mechanics*, Vol. 9, No. 4, (2016), 1135-1146.
  21. Sabour, M., Ghalambaz, M. and Chamkha, A., "Natural convection of nanofluids in a cavity: Criteria for enhancement of nanofluids", *International Journal of Numerical Methods for Heat & Fluid Flow*, Vol. 27, No. 7, (2017), 1504-1534.
  22. Iwatsu, R., Hyun, J.M. and Kuwahara, K., "Mixed convection in a driven cavity with a stable vertical temperature gradient", *International Journal of Heat and Mass Transfer*, Vol. 36, No. 6, (1993), 1601-1608.

## A Characteristic-based Numerical Simulation of Water-titanium Dioxide Nano-fluid in Closed Domains

T. Adibi<sup>a</sup>, S. E. Razavi<sup>b</sup>, O. Adibi<sup>c</sup>

<sup>a</sup> Department of Mechanical Engineering, University of Bonab, Bonab, Iran

<sup>b</sup> School of Mechanical Engineering, University of Tabriz, Tabriz, Iran

<sup>c</sup> School of Mechanical Engineering, Sharif University of Technology, Tehran, Iran

### P A P E R I N F O

چکیده

#### Paper history:

Received 19 September 2019

Received in revised form 04 November 2019

Accepted 08 November 2019

#### Keywords:

Titanium Dioxide

Nano-fluid

Nusselt Number

Friction Factor

Numerical Method

یک روش پایه مشخصه برای حل همرفت اجباری و ترکیبی بسط داده شد. جریان نانو سیال با روش پایه مشخصه بسط داده شده، در فضای بسته با نسبت منظری های مختلف شبیه سازی شد. برای این منظور، کدی در نرم افزار فرترن نوشته شد. آب به عنوان سیال خالص و آب به همراه دی اکسید تیتانیم به عنوان نانو سیال در نظر گرفته شد. معادلات حاکم بر جریان با روش حجم محدود و جملات همرفت با روش پایه مشخصه حل شدند. شبیه سازی ها برای گستره بزرگی از اعداد رینولدز و گراشف و همچنین برای کسر حجمی و نسبت منظری های مختلف انجام شد. خطوط جریان، خطوط دما ثابت، ضریب اصطکاک و عدد ناسلت در شرایط مختلف تعیین شد. رفتار همرفت نانو سیال به صورت تابعی از پارامترهای مختلف مثل عدد گراشف و نسبت منظری تعیین شد. نتایج نشان داد عدد ناسلت متوسط برای نانو سیال در قیاس با آب تا ۲۳٪ افزایش نشان می دهد.

doi: 10.5829/ije.2020.33.01a.18